

# XPS and HAXPES of compressed MXene aerogels

**Date:** 2022-02-01

**Tags:** Freeze-cast Nanoplexus 400 2021 Calendering Aerogel 06/12/2021Synth KTH Collab Nanoplexus Ti3C2Tz 2021 XPS HAXPES

**Created by:** James Bird

---

**Goal : Use X-ray photoelectron spectroscopy and Hard X-Ray Photoelectron Spectroscopy to derive a semi-quantitative estimate of  $\text{Ti}_3\text{C}_2\text{T}_z$  MXene terminating group stoichiometry and sample purity**

## Materials:

Samples produced in [Experiment - Calendering of freeze-cast MXene aerogel IV](#), hence freeze-cast, lyophilised, calendared  $\text{Ti}_3\text{C}_2\text{T}_z$  MXene aerogels of dimensions 10 x 10 x 1.25 mm, with a rough density of  $1.23 \text{ gcm}^{-3}$ .

## Procedure :

Hard X-ray Photoelectron Spectroscopy (HAXPES) is performed using monochromated Ga  $\text{K}\alpha$  metal jet X-ray radiation (9252 eV, 3.57 mA emission at 250 W, micro-focussed to 50  $\mu\text{m}$ ) and an EW-4000 high voltage electron energy analyser (HAXPES-Lab, Scienta Omicron GmbH); the instrument has a base vacuum pressure of  $5 \times 10^{-10}$  mbar. The entrance slit width used was 1.5 mm, and the pass energies used for survey and core level spectra were 500 and 100 eV respectively, with total energy resolutions of 2.0 and 0.6 eV respectively. Detector angle at  $90^\circ$  to sample normal.

The HAXPES instrument also has a monochromated Al  $\text{K}\alpha$  X-ray source (1486 eV, 20 mA emission at 300 W) for surface sensitive XPS at the same sample position. Charge neutralisation for insulating samples is achieved using a low energy electron flood source as required (FS40A, PreVac). Core level relative sensitivity factors for HAXPES quantification were calculated according to references, and are captured in CasaXPS-GaKa1.lib. Detector angle at  $60^\circ$  to sample normal.

## Analysis:

Using Casa XPS v2.3.25 for all data analysis. Library is Scofield (casaXPS-scofield.lib) for conventional XPS and CasaXPS-GaKa1.lib for HAXPES.

## Wide Scan Surveys - Quantification

- Calibrate according to Natsu2021, such that Ti-C-Ti species peak is at 282.0 eV (described more below).
- HAXPES with -0.7 KE Exp. correction and input ADC Angle of 90 degrees. Regions added for C 1s, Ti 1s, O 1s, F 1s and Cl 1s with U 2 Tougaard background and average region width either 1 or 5 dependent on need to avoid adjacent peaks or not, respectively.
- XPS with -0.7 KE Exp. correction and input ADC Angle of 60 degrees. Regions added for C 1s, Ti 2p, O 1s, F 1s and Cl 2p with U 2 Tougaard background and all average region widths 5.
- An alternative escape depth correction was also used for quantification of the survey scan of conventional XPS data, where CH film escape depth correction is used to return  $Ti_3C_2$ , requiring values for MFP Exp of 40.7 and 43.7 for the unheated and heated samples, respectively.

## Element scan regions

- Cl 2p are not fit due to absence of information in the literature
- HAXPES-only Ti 1s & Cl 1s regions are also not deconvoluted for the same reason

## Titanium 2p

Attempts were made to fit the data according to Schultz2021, Natsu2021 & Persson2017, with the best results being given largely by a fit to Schultz et al.'s work. The initial goal was to derive the fit by constraining the higher BE orbit-split peaks with relation to each of their lower energy pairs i.e. by spacing, FWHM and area constraints. All MXene-related metallic peaks fit with asymmetric peaks and refinements to peak model made using 'Test Peak Model' function, whilst keeping  $TiO_xF_{4-2x}$  fit as GL(30) symmetric peak. The lower BE of each spin-orbit doublet is constrained by fwhm only, to match the range found in the literature: 0.7-1.1, 1.2 or 1.4 eV for the MXene-corresponding peaks in order of increasing BE, and 1.0-2.0 eV for the  $TiO_xF_{4-2x}$  peak. Each higher energy peak of a spin-orbit coupled pair is then constrained to have the half area of its lower BE pair. The BE spacings in each doublet are set at 5.9, 5.4, 5.4 (Schultz2021) and 5.7 eV (Benchakar2020) and the fwhms are set at 2, 1.72, 1.72 (Persson2017) and 1.81 (Benchakar2020) times their lower BE pair. Using this model, every BE doublet peak is either at, or just below, the maximum possible fwhm within the constraint. No position restraints are required nor used.

## Carbon 1s

C1s fitting was initially problematic - it seemed necessary to fit five peaks with constraints: one asymmetric for Ti-C-Ti, three presumed to be C-C, C-O and C=O symmetric peaks and an extra unknown in between the large C-C and smaller Ti-C-Ti in the peak bridging region. This latter peak is fwhm-matched with all other presumed non-metallic peaks, which found values of 1.5 eV for FWHM. In this scenario, adventitious carbon is seemingly at 285.4 eV, much greater than the regularly cited 284.8 eV.

When propagating the above regions and refitting, in one instance the bridging peak disappeared to give zero area. On the basis of this finding, a new model was explored on the basis of Greczynski2021, and general literature around the difficulty of finding a reliable binding energy for adventitious carbon. Of utmost importance is achieving a good calibration, hence the fit was optimised by adjusting the line shape of the Ti-C-Ti asymmetric peak and a fitting a single symmetric peak (GL30) to the adventitious carbon (AdC). Of course, the actual AdC peak consists of subcomponents, but with the emphasis on achieving a good calibration, this is entirely unimportant. Qualitatively, it is apparent that the HAXPES analysis gives a lower proportion of AdC to Ti-C-Ti, as expected.

## Fluorine 1s

Two-peak model expounded by Schultz2019 gives 685.1 and 685.2 for XPS and HAXPES data for the Ti-F peak location, respectively, when constraining FWHM values to equivalent. These values correspond well with the literature. The impurity peak however is inconsistently located at 686.0, 686.3, 686.4 and 687.1. The single peak model (Natu2021) gives the same peak locations described above, and does not present this additional inconsistency. Additionally, in the absence of Li or Al detection, this model is reasonable.

## Oxygen 1s

With O1s fitting, the decision was made to go slightly rogue after inspecting the body of literature and finding minimal consistency, even despite the review by Natu et al. Again, qualitatively, it can be seen from comparing the HAXPES data with the XPS that the higher binding energy region and 'bump' must correspond to any contaminants, considering its reduced intensity in the HAXPES. After trying to fit using Schultz2021, Natu2021 & Persson2017, no overall fit was convincing, considering the severity of the constraints that needed applying. Namely, no fit would consistently locate a second or additional Ti-O MXene peak within the lower

binding energy hump which corresponds to a Ti-O bonding environment, other than that at 529.9 eV. The region instead where a second peak naturally refines to in a three-peak model is in the region 530.9-531.0 eV, which from Natsu et al. corresponds to  $\text{TiO}_{2-x}\text{F}_x$ . It is already known from the fit of Ti 2p region that there is indeed an atypically prominent peak in the  $\text{TiO}_{2-x}\text{F}_x$  region, accounting for  $15.09 \pm 1.27$  % by area/concentration. The presence of  $\text{TiO}_2$  when the measurement was made is entirely unsurprising considering the time between synthesis and analysis of nearly two months, despite attempts to preserve sample stability. Hence, a three-peak model was devised, where the Ti-O MXene peak at 529.9 eV is fit with an asymmetric peak to account for its metallic nature, a second symmetric peak is placed at 530.9-531.0 eV and its area constrained to 25% of the Ti-O MXene, and a third symmetric peak, simply labelled AdO for adventitious oxygen is added to capture the higher binding energy region. The fits are consistently excellent, and no advantage was found in deconvoluting the adventitious oxygen peak further. AdO peaks are centered between 532.1-532.5 eV.

The 25% relative area is defined by calculating the average proportion of each Ti 2p peak assigned to Ti-O MXene bonds for each scan, hence 100% of the fraction at 455.0-455.2 eV (Ti-O/O/O) and its doublet pair, 2/3 of the fraction at 456.0-456.1 eV (Ti-O/O/F) and its doublet, and 1/3 of the fraction assigned at 457.1-457.2 eV (Ti-O/F/F). These sum to give  $60.65 \pm 1.12$  %, which relative to the  $15.09 \pm 1.27$  % registered as  $\text{TiO}_{2-x}\text{F}_x$ , is roughly four times. It must again be noted, that the model expounded by Natsu et al. whom identified an additional Ti-F/F/F bonding environment in the Ti 2p peak was dysfunctional for this dataset.

## Results :

Raw data is in the .vms file, named JB\_MXene\_Jan22.vms and analysed data are in jb\_mxene\_jan22\_analysisv2.vms. Untreated sample data exports are all of filetype .csv, with a filenames convention (FNC) of: all JB\_Untreated\_\_Sect\_Sect\_0001.csv, where is either HAXPES or XPS, and is the name of any of the deconvoluted peaks C\_1s, O\_1s, Ti\_2p or F\_1s. All sample data exports are also of filetype .csv, and use the FNC of Report\_.csv, where is as before, but with the addition of 'Wide' for the wide scan ranges (surveys). A plot of all the deconvoluted peaks, comparing XPS (top row) and HAXPES (bottom row) are produced using the Python script XPSvsHAXPES.py (available on Github).

Calibration as described accorded well with Fermi level calibration, although in some cases the zero-energy transition is unclear, hence why the calibration to Ti-C-Ti was selected across all scans.

Using the kinetic energy exponent escape energy correction, HAXPES overall compositions of the near-surface region of the untreated and heat-treated aerogels are found to be  $\text{Ti}_3\text{C}_{2.89}\text{O}_{0.737}\text{F}_{0.486}\text{Cl}_{0.255}$  and  $\text{Ti}_3\text{C}_{1.7}\text{O}_{0.484}\text{F}_{0.313}\text{Cl}_{0.153}$ , respectively, where Ti stoichiometry is scaled to equal three. Conventional aluminium source XPS returns  $\text{Ti}_3\text{C}_{10.1}\text{O}_{1.95}\text{F}_{1.19}\text{Cl}_{0.406}$  and  $\text{Ti}_3\text{C}_{11.6}\text{O}_{2.11}\text{F}_{1.1}\text{Cl}_{0.419}$  for the untreated and treated samples, respectively. Using the CH film escape depth correction instead for the conventional XPS data gave compositions of  $\text{Ti}_3\text{C}_2\text{O}_{4.22}\text{F}_{25.2}\text{Cl}_{0.0432}$  and  $\text{Ti}_3\text{C}_2\text{O}_{4.86}\text{F}_{29.5}\text{Cl}_{0.0333}$  for the untreated and heat-treated aerogels, respectively.

The peak locations, fwhms and fractions are slightly different across the HAXPES and XPS samples, as summarised below.

### XPS summary

Region	BE (eV)	FWHM (eV)	Fraction	Assigned to
Ti 2p <sub>3/2</sub> (2p <sub>1/2</sub> )	455.2 (461.0)	0.9-1 (1.9-2.0)	0.31	C-Ti-(O/O/O)
	456.0-456.1 (461.4)	1.2 (2.1)	0.32	C-Ti(O/O/F)
	457.1-457.2 (462.5-462.6)	1.4 (2.4)	0.23	C-Ti(O/F/F)
	459.0-459.2 (464.7-464.9)	1.9 (3.4-3.5)	0.14	TiO <sub>2-x</sub> F <sub>2x</sub>
C1s	282.0	0.6	0.26	Ti-C-Ti
	285.5-285.6	1.6-1.7	0.74	AdC
O1s	529.9	0.8-0.9	0.40	C-Ti-O
	530.9	1.0-1.1	0.10	TiO <sub>2-x</sub> F <sub>2x</sub>
	532.4-532.5	3.2-3.3	0.50	AdO
F1s	685.2	1.3	1	C-Ti-F/TiO <sub>2-x</sub> F <sub>2x</sub>

### HAXPES summary

Region	BE (eV)	FWHM (eV)	Fraction	Assigned to
Ti 2p <sub>3/2</sub> (2p <sub>1/2</sub> )	455.0-455.1 (460.9-461.0)	1.1 (2.2)	0.35	C-Ti-(O/O/O)
	456.0-456.1 (461.4)	1.2 (2.0)	0.31	C-Ti(O/O/F)
	457.2 (462.6)	1.4 (2.4)	0.19	C-Ti(O/F/F)
	459.2 (464.9)	2 (3.6)	0.16	TiO <sub>2-x</sub> F <sub>2x</sub>
C1s	282.0	1.0-1.1	0.38	Ti-C-Ti

	285.4-285.5	1.8	0.62	AdC
O1s	529.9	1.2	0.51	C-Ti-O
	530.9-531.0	1.0-1.2	0.13	TiO <sub>2-x</sub> F <sub>2x</sub>
	532.1-532.2	3.3-3.4	0.36	AdO
F1s	685.1	1.5-1.6	1	C-Ti-F/TiO <sub>2-x</sub> F <sub>2x</sub>

On removing the fractions considered impurities for each element (non-native to MXene), in combination with the overall concentration of each element obtained from the survey scan (Report\_Wide.csv), we can arrive at estimates for the stoichiometry of the MXene alone (T\_zQuant.xlsx). For each untreated sample, the stoichiometries are hence  $\text{Ti}_3\text{C}_{1.29}\text{O}_{0.44}\text{F}_{0.57}\text{Cl}_{0.3}$  and  $\text{Ti}_3\text{C}_{3.05}\text{O}_{0.91}\text{F}_{1.39}\text{Cl}_{0.47}$  for HAXPES and XPS samples, respectively, when scaling so that the Ti atom ratio is 3.

## Discussion :

Moeity definitions generally follow those as described in Natu2021, with the exception of the impurities discussed earlier. An obvious exception is the lack of the C-Ti-(F/F/F) moiety in Ti 2p analysis. Its absence is however unsurprising considering the fitting method used here, where positions are not defined previously, such that a low fraction of just 4% (as given in the article) would only appear with notable constraints.

The suggestion of the survey scan quantification is clear when using the kinetic energy exponent escape depth correction: much adventitious carbon is being detected in conventional XPS, whilst there is significantly less detected with HAXPES. The attempt to correct for CH impurities in conventional XPS with the CH film correction does not however provide an accurate alternative representation to correlate with the HAXPES quantification of composition, as a dramatic excess of fluorine and oxygen is calculated. Indeed, less oxygen associated with adventitious carbon is seen in the HAXPES O 1s spectrum, as well as less adventitious carbon in the C 1s peaks. An exception however arises on inspection of the F 1s peak, where the relative amount of the impurity-correlated peak (Schultz2019) in a two-peak model seems to increase in HAXPES.

The fluorine excess would point to poor washing, and hence an inability to remove Al and Li also. In the absence of an aluminium peak there may be LiF remaining. This cannot be confirmed directly through quantification of the LiF peak due to the overlap of Ti 3s and Li 1s (the only transition for Li). Microanalysis results of the same material ([Experiment - Microanalysis of MXene synthesis products I](#)) however



suggest  $< 1$  wt% Li. So although there maybe fluorine impurities remaining, when considering the [LiF]/[MAX] initial molar ratio is 11.9 ([Experiment - MXene synthesis XI](#)), even in the instance where all aluminium is etched and converted into  $\text{AlF}_3$ , the [LiF]/[MXene] molar ratio maximum is limited to 8.9. Hence the CH film method of escape depth correction is however certainly flawed for this sample type, as the microanalysis data and does not correlate with these quantities.

On the basis of unclear salt impurity presence, the F 1s element scan region is more suitably assigned as a single asymmetric Ti-F peak (Natu2021). Amongst four of the elemental peak scan ranges, there does occasionally appear to be shoulders on the high BE side of the F 1s peak, and seemingly no single lineshape model of peak asymmetry perfectly captures the peak shape in the absence of a smaller, higher BE impurity peak. It can be noted from the peak fitting however that fluorine seems to exist in three separate bonding environments, which of course are not resolved in this model.

Although Cl 2p peaks are not fit, the untreated sample in HAXPES gives no clear peak, and the treated sample a much smaller peak(s) than either of the conventional XPS samples ( $< 20$  vs  $< 65$  cps). Despite this, the Cl 1s peak is evident in both HAXPES measurements, although with significant asymmetry indicating either metallic bonding and/or multiple bonding environments. Chlorine in microanalysis accounts for  $\sim 4.6$  wt% in excellent agreement with HAXPES and XPS which find 4.3 wt%.

If the peak convolutions and moiety assignments are reasonable, then the issues of C stoichiometry not being 2 and  $\Sigma z$  also not being equal to 2 for the MXene stoichiometry quantification instead points to an issue with the quantification of the survey scan - notably, although both an angular distribution correction and an escape depth correction are applied and the correct library for each system selected, there is no transmission function (or correction) applied due to their unavailability. That being said, the concentrations measured in HAXPES correlate well overall to the microanalysis result of the same material ([Experiment - Microanalysis of MXene synthesis products I](#)), which would point instead to a poor moiety definition and spectrum deconvolution.

## Conclusions :

An overall suitable, adequate and convincing description of the bonding environment for each element is found, with each environment described in the literature. Fractions of each moiety do not match so well to the literature, although

such a finding is understandable given the delay between synthesis and measurement and hence the notable oxidation and adventitious carbon and oxygen build-up. The key finding is that the outcome of the HAXPES analysis differs minimally from the XPS analysis, with the exception of the difference in adventitious impurities, suggesting the impurities are indeed correctly defined and are located on or closer to the surface. The work hence demonstrates that sputter-cleaning can, and should be avoided in conventional XPS measurements (as performed in Halim2016) to ensure no sputter damage is introduced.

## Linked experiments

Success - [MXene synthesis XI](#)

Success - [Calendering of freeze-cast MXene aerogel IV](#)

Success - [Microanalysis of MXene synthesis products I](#)

## Attached files

CasaXPS-GaKa1.lib

sha256: 3ef2f5dce41b28dd10f9f73b8450cc03759109b4101ad06f918ebaf63859ec7d

all\_JB\_Untreated\_XPS\_F\_1s\_Sect\_Sect\_0004.csv

sha256: 4bf36b8e89c61b3e23de4cc1fec8577199abe25e94a5a01120eddc2941d4cca4

all\_JB\_Untreated\_XPS\_O\_1s\_Sect\_Sect\_0006.csv

sha256: 016bb37a1fad558063c81d5732495922dcd979dce9efb72cd0c0b0ce919d38e8

all\_JB\_Untreated\_XPS\_Ti\_2p\_Sect\_Sect\_0008.csv

sha256: e91fbcc74afdfd137f4734e80ff8043dbb73387a5409f86943a1f8d682308537

all\_JB\_Untreated\_HAXPES\_C\_1s\_Sect\_Sect\_0001.csv

sha256: cf2da453b43180a49888b06fef7e30916b4e120d7455d7200814c1098f69fdeb

all\_JB\_Untreated\_HAXPES\_F\_1s\_Sect\_Sect\_0003.csv

sha256: acaec10e2a61d057bef9518f8d3159ef7ac23869dfff144c5e78f8d998f1a82f

all\_JB\_Untreated\_HAXPES\_O\_1s\_Sect\_Sect\_0005.csv

sha256: 83bc969a9d01feb4192f62e0903fd285a779fa48832226347fde74b9ef1efd58

all\_JB\_Untreated\_HAXPES\_Ti\_2p\_Sect\_Sect\_0007.csv

sha256: c9e9d56a80f71537bc783dcc1bd1f0381b40e61571cf27ee8622d568a6bf0da7

all\_JB\_Untreated\_XPS\_C\_1s\_Sect\_Sect\_0002.csv



sha256: 9ff9bbd5295f033b701dcbcb6dcad8ae23dba242c2d7fdd90285886915161b2b9

Report\_Ti2p.csv

sha256: e109cdef89cb72af2f2c7e552ea0ae53eac0d150015b3326a0c12db9ad52d10d

Report\_Wide.csv

sha256: 48cd33f7a9df0a47302051229e2241ad4069eae880507dc926e28883773b71bc

Report\_C1s.csv

sha256: b292a7fcc318cfca60f12ac50f3b25da2bb48b2e34b486b88aa1e9acf9d8c26f

Report\_F1s.csv

sha256: 479664f3672ea82018792f8b99f2e87a4451a10c22e7e91739a6aeda64a71e0f

Report\_O1s.csv

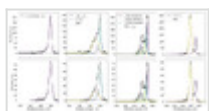
sha256: 85f1ef54b07dd516511650916d8159d205d8a309fb58705ef33cae12f66ff0f8

Tz\_Quant.xlsx

sha256: 429784fc8864b9061ff967d175b0318c8f95b9ff593c621c51bba13253460315

HAXPESvsXPS.png

sha256: 081d2c0dbd08229f438d6e50043be5fdf5510d57086c97d983411e0bb25365e7



JB\_MXene\_Jan22.vms

sha256: 2ae981c3c9af57363e4415f06d59b9964c0d96a59f37d94b02ab9e6f78cd5fa7

jb\_mxene\_jan22\_analysisv2.vms

sha256: 51e479ae33c4047ea906147b68b9562213f67b769eac8e48d800449f22f63652



Unique eLabID: 20230730-c5493f119c2030e3e703ad6bf3067b508e000dd1

Link: <https://frankel-elab.manchester.ac.uk/experiments.php?mode=view&id=141>